



LJMU Research Online

Wei, J, Hou, X, Xu, G, Zhang, G and Fan, H

Modeling and machining of integral impeller based on NURBS curve

<http://researchonline.ljmu.ac.uk/id/eprint/14508/>

Article

Citation (please note it is advisable to refer to the publisher's version if you intend to cite from this work)

Wei, J, Hou, X, Xu, G, Zhang, G and Fan, H (2021) Modeling and machining of integral impeller based on NURBS curve. International Journal of Advanced Manufacturing Technology. ISSN 0268-3768

LJMU has developed **LJMU Research Online** for users to access the research output of the University more effectively. Copyright © and Moral Rights for the papers on this site are retained by the individual authors and/or other copyright owners. Users may download and/or print one copy of any article(s) in LJMU Research Online to facilitate their private study or for non-commercial research. You may not engage in further distribution of the material or use it for any profit-making activities or any commercial gain.

The version presented here may differ from the published version or from the version of the record. Please see the repository URL above for details on accessing the published version and note that access may require a subscription.

For more information please contact researchonline@ljmu.ac.uk

<http://researchonline.ljmu.ac.uk/>

Modeling and Machining of Integral Impeller based on NURBS Curve

Juan Wei¹, Xiaodong Hou¹, Chao Sun¹, Guipeng Xu¹, Guangming Zhang², Hongwei Fan

(¹College of Mechanical Engineering, Xi'an University of Science and Technology, Xi'an 710054, China)

(²Faculty of Engineering and Technology, General Engineering Research Institute, Liverpool John Moores University, Liverpool, L3 3AF, United Kingdom)

Correspondent author: Juan Wei, E-mail: juanw@xust.edu.cn

Abstract: NURBS curve is applied to model and machine of integral impeller to get better smooth streamline in this work. In order to get high precision surface modeling of impeller, complex surface modeling method for impeller is studied through inputting NURBS curves and surfaces obtained by MATLAB into CAXA Manufacturing Engineer, which solves the problem that cannot be designed NURBS curve and surface directly in the CAD software. Grooving and expanding groove tool paths are obtained according to the NURBS curve of top curve and root curve, and its interpolation step size and the row spacing are determined according to the curvature of the curve and interpolation period. Meanwhile, Five-axis side milling method is used to achieve the vane finish machining, and streamline processing method is adopted to realize the finish machining of the channel. All work is verified in a virtual simulation system of 5MC850-C machining center, and these simulation results show that machining accuracy error of the impeller is between -0.007 mm and 0.012 mm, meeting tolerance range of the impeller design.

Keywords: Five-axis linkage; Integral impeller; NURBS curve; Grooving curve; Expanding groove; Simulation verification

1. Introduction

Nowadays, integral impeller is widely used in energy field, defense and aerospace field, which plays an extremely important role in reducing weight, enhancing performance and improving reliability of the engine [1]. The structure of the integral impeller mainly includes hub and vanes, in which each vane consists of leading edge, trailing edge, pressure surface and suction surface. The hub and vanes profile are usually free-form surfaces, the vanes are very complex twisted with overlapped each other, and the channel is narrow [2]. Thence, the design of integral impeller must not only meet the requirements of high aerodynamics and surface accuracy, but also avoid collision and interference between the tool and the workpiece during the processing [3, 4]. Currently, the modeling and processing of integral impeller have been the research focus of domestic and foreign scholars. Non-Uniform Rational B-Spline (abbr. NURBS) can better control curvature and its variation of complex surface than the traditional grid modeling method, so it can create more realistic and vivid modeling. And ISO has used NURBS as the only mathematical method for defining

36 geometry of industrial products [5]. Therefore, it is of great significance to study integral impeller surface
37 modeling and processing technology based on NURBS curves, use NURBS curves to generate impeller
38 profiles and tool planning paths for impeller machining, and develop interpolation algorithms based on
39 NURBS curves.

40 In traditional five-axis machining, a large number of small linear segments or arcs are used to represent
41 the processing path, which increases the data processing quantity of the numerical control system and fails
42 to realize the optimal smooth effect of the surface, and processing effect is often affected by the nonlinear
43 error, resulting in poor machining surface quality[6,7]. In theory, non-linear errors can be eliminated using
44 NURBS describe the tool center point and tool axis point trajectory, thus a higher and smoother feed speed
45 can be obtained, frequent machine acceleration and deceleration can be reduced, and high-speed and high-
46 precision machining can be achieved[8]. For five-axis CNC machining of an impeller, many studies have
47 been performed on the tool path planning in recent years. Fan et al.[9] presented a novel five-axis rough
48 machining tool path by mathematical analysis and comparing between free-form vane and ruled vane. Kim
49 et al.[10] introduced a new method of machining impellers by integrating 3-axis and 5-axis machines, which
50 can reduce significantly up to 17% of total machining time. Chen[11] put forward a method of the optimal
51 tool orientation in a five-axis flank milling machine, claiming that the tool orientation can be ensured by a
52 mathematical formula and CAD/CAM software Unigraphics (UG), and the tool path can be transformed into
53 the NC code. The machined impeller surface geometry is used to verify accurately by using the 3D
54 Coordinate Measuring instrument. Wang et al.[12] presented a method that knowledge engineering
55 technology was introduced into the computer numerical control programming, and a standard process
56 template was established for the processing of impeller parts. Han et al.[13] proposed a path planning method
57 based on template path mapping for impeller channel, and the tool path calculation time is compared with
58 the traditional equidistant offset method, resulting in 45% increase in computing efficiency.

59 Aiming at NURBS curve interpolation technology, Li et al.[14] introduced a third-order non-uniform
60 rational b-spline interpolation method. This method can create a smooth transition between the hub and the
61 blade shoulder and is implemented in an open structure computer numerical control controller. Wu et al.[15]
62 proposed a tool preprocessing method for high-speed processing based on NURBS curve fitting technology
63 in order to improve the processing quality while reducing the processing time. Liu et al.[16] put forward a
64 NURBS tool path interpolation method for reducing the feed fluctuation by forming a quartic equation for
65 the curve parameter increments. Yao et al.[17] proposed a method of eliminating non-linear errors by five-
66 axis linkage double NURBS curve direct interpolation to control non-linear errors.

67 The aforementioned literatures reveal theoretical studies on the tool path planning and interpolation
68 algorithms of integral impeller. However, few studies have applied NURBS curves to the modeling, tool
69 path and interpolation synthetically, whereby the mathematical analysis should be carried out and calculation
70 method must be proposed. There are two problems that must be addressed in this methodology: modeling,
71 tool path planning and interpolation method of impeller based on NURBS curve surface, and the machining
72 parameters of interpolation step and interpolation period that should be considered based on NUBRS tool
73 path.

74 The objective of our work is to resolve the two above-mentioned issues in a scientific way. Firstly,
 75 impeller model is generated using NURBS curves and surfaces, tool paths are got based on the NURBS
 76 model of the impeller, and machining processing is realized by NURBS interpolation method. Secondly,
 77 rough machining method for separating grooving and expanding groove is presented to reduce and release
 78 residual stress and elastic potential energy better. Thirdly, a five-axis machining center virtual simulation
 79 system is established, and the design model, blank model and tool path file of impeller are imported into it
 80 for numerical control machining simulation verification. The results show that our work is feasible and the
 81 machining error was between $-0.007mm$ and $0.012mm$, which can meet the design requirements.

82 2. Modeling and machining of NURBS curve and surface

83 NURBS curve has the advantages of excellent local shape control force and geometric non-deformation, and
 84 is significantly convenient for engineering application. Therefore, NURBS curve and surface are used to
 85 realize the modeling vanes profile and hub surface, and NURBS curve interpolation is adopted to machine
 86 the channels and the vanes of the integral impeller.

87 2.1 Modeling of vane profile and hub surface

88 As mentioned earlier, the integral impeller is composed of the hub and the vanes, in which the vane top line
 89 and vane root line are given in the form of list points. The equations of vane top line and vane root line based
 90 on NURBS curve $C(u)$ can be expressed as follows[18-20].

$$91 \quad C(u) = \frac{\sum_{i=0}^n W_i N_{i,k}(u) P_i}{\sum_{i=0}^n W_i N_{i,k}(u)} \quad (1)$$

92 where n is the number of list points; k is the number of times of the NURBS curve, here $k=3$; $W_i (i=0,1,2,\dots,n)$
 93 is the weight factor of the i th control point P_i , here $W_i > 1$; P_i is the i th 3D control vertex. $N_{i,k}(u)$ is the i th B-
 94 spline basis function, which is defined as follows.

$$95 \quad N_{i,0}(u) = \begin{cases} 1 & u \in [u_i, u_{i+1}) \\ 0 & other \end{cases}$$

$$N_{i,k}(u) = \frac{u - u_i}{u_{i+k} - u_i} N_{i,k-1}(u) + \frac{u_{i+k+1} - u}{u_{i+k+1} - u_{i+1}} N_{i+1,k-1}(u)$$

$$\frac{0}{0} = 0 \quad \text{regulations}$$

96 The vane profile uniformly distributed on the impeller hub is a non-developable ruled surface, which is
 97 produced by a rule line along two leading lines according to the equal parameter method, here the two leading
 98 lines are the vane top line and the vane root line on the same side of the vane. The hub surface is a rotating
 99 surface formed by a vane root line around the impeller axis. Therefore, the vane profile and the hub can be
 100 expressed as[21, 22]:

$$S(s, t) = \frac{\sum_{i=0}^m \sum_{j=0}^n N_{i,3}(s) N_{j,3}(t) w_{ij} G_{ij}}{\sum_{i=0}^m \sum_{j=0}^n N_{i,3}(s) N_{j,3}(t) w_{ij}} \quad (2)$$

where $S(s, t)$ is the position vector of any point on NURBS surface, $N_{i,3}(s)$ and $N_{j,3}(t)$ are cubic b-spline basis functions along s and t directions, respectively, w_{ij} is the weight factor, G_{ij} is the control point.

NURBS surface is a segmented surface, which only local description information is involved in any of the surface slices. Therefore, the following expressions of NURBS surface slices in matrix form can be obtained by appropriate transformation of equation (2).

$$\begin{aligned} x(u, v) &= UM_u G_x M_v^T V^T / UM_u WM_v^T V^T \\ y(u, v) &= UM_u G_y M_v^T V^T / UM_u WM_v^T V^T \\ z(u, v) &= UM_u G_z M_v^T V^T / UM_u WM_v^T V^T \end{aligned} \quad (3)$$

where $x(u, v)$, $y(u, v)$ and $z(u, v)$ are x , y and z coordinates of any point $S(u, v)$ on the surface, u and v are the transformed variables, $U = [u^3 \ u^2 \ u]$, $V = [v^3 \ v^2 \ v \ 1]$. M_u and M_v are the node coefficient matrices of the surface slice, which are determined by the node vectors of u -direction and v -direction, respectively. W is the weight factor matrix of the surface slice. G_x , G_y and G_z are the geometric coefficient matrix of the surface slice.

2.2 NC Machining of Impeller based on NURBS Curve

Conventional NC machining method of the free-form surface is to generate the tool position file describing tool path by off-line programming according to the geometric information of the surface and the machining process information. The NC program of the part is obtained through the post-processing, and after simulation verification the NC program is input NC machine tool for machining. This process mainly depends on the programmer, which not only has a large amount of programming workload and subjective factors but also has more redundant procedures and consumes more software and hardware resources. At the same time, because of the separation of tool path planning and trajectory generation, it is difficult to realize 3D real-time and accurate tool compensation, which causes machining and programming to be carried out alternately multiple times, and seriously affects NC machining efficiency and surface machining accuracy.

NURBS surface modeling and interpolation method of impeller model-based definition is proposed in our work, it consists of channel grooving, expanding groove tool path generation and direct interpolation based on NURBS curve modeling technology, calculate maximum tool radius according to curvature of curve, and design NUBRS curve interpolator to realize the machining of integral impeller. The flowchart of the method is shown in figure 1.

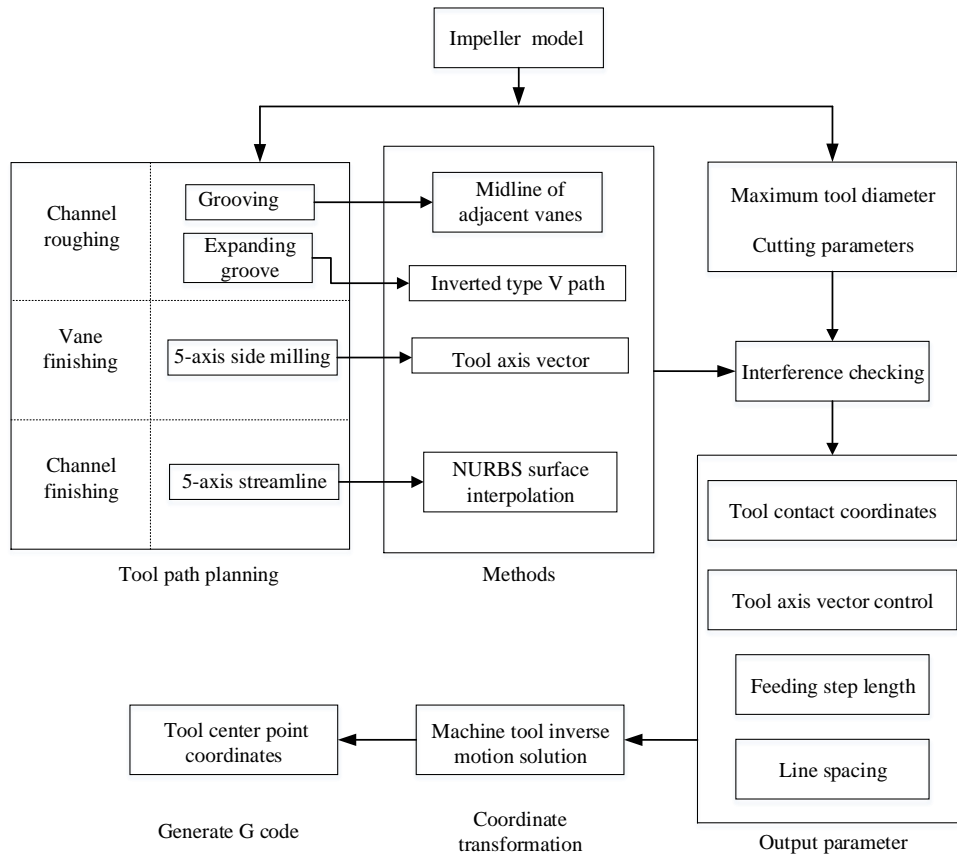


Fig. 1 Machining process of integral impeller

127 Because the integral impeller is forged, there is not only a large amount of machining allowance to be
 128 removed, but also residual stress and elastic potential energy need to be released before and during machining,
 129 so the machining technology of the integral impeller is particularly important to the machining accuracy and
 130 efficiency of the impeller. In order to remove the residual stress and elastic potential energy in the impeller
 131 blank at the earliest of process, rough machining process is proposed, in which the channel is grooved first,
 132 and then the groove is enlarged. Grooving line and expanding groove line are both NURBS curves, which
 133 are generated according to the NURBS curve of the vane profile. Five-axis side milling method is adopted
 134 for the finish machining of the vane profiles, and the non-developable ruled surface on both sides of vanes
 135 profile is realized by controlling the direction of the tool axis. Finish machining of the channel is
 136 implemented using a five-axis streamline processing mode, milling from the inlet to the outlet of the channel.

137 3 Planning of NC machining tool path

138 3.1 Tool path planning of the channel rough machining

139 A uniform stratification processing strategy is adopted in the rough machining of channels. Tool path for
 140 each layer cutting is connected in a proper way, forming the whole machining tool path of the channel. Cross-
 141 section of channel is an approximate trapezoid with a narrower inlet and a wider outlet, thus, the inverted V-
 142 type tool path is used. First a through groove is processed in the middle of a channel, then inverted V-shaped
 143 expanding groove tool paths are planned on the two sides. The tool path of each layer is basically the same.

144 **3.1.1 Grooving process of channel**

145 Main purpose of grooving is to open the channel, release the forging stress and potential energy in the process
 146 of machining, and prepare for the subsequent machining such as expanding groove. This work is finished
 147 using flat end milling tool, grooving position is selected in the middle position of channel, and milling
 148 direction from inlet to outlet of impeller. Grooving machining includes determination of grooving line,
 149 calculation of feed step size and selection of diameter of milling tool.

150 Figure 2 shows a grooving tool path of one of the layer cuttings. E_1 and E_2 are two boundary-lines of
 151 channel rough machining, and are obtained by offsetting a distance away from designed vane curve V_1 and
 152 V_2 , the distance is the allowance for finish η respectively. OB is a grooving path located in the middle
 153 position of E_1 and E_2 , which can be expressed in formula (4).

154
$$C_{BO}(u) = \frac{\sum_{i=0}^n W_i N_{i,k}(u) P_{BO,i}}{\sum_{i=0}^n W_i N_{i,k}(u)} \quad (4)$$

155 where $P_{BO,i}$ can be obtained by control point and data point $p_{BO,i}$ relationship (15). Thus, $p_{BO,i}$ data point
 156 is figured out [23, 24].

157
$$p_{BO,i} = \begin{bmatrix} \cos \theta & -\sin \theta & 0 \\ \sin \theta & \cos \theta & 0 \\ 0 & 0 & 1 \end{bmatrix} p_{V_1,i}$$

158 Where $p_{V_1,i}$ is data points on V_1 . θ approximately equal to $360/2n$. n is the number of vanes.

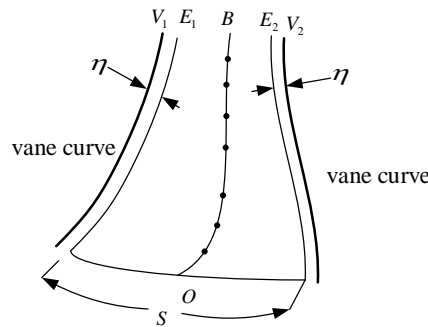


Fig. 2 Determination of grooving path

159 Feed step size is calculated to control moving distance of tool relative to workpiece in an interpolation
 160 period. Planned grooving tool path is located on machined surface with a time-independent geometric path,
 161 which is described into a series of tool contacts point according to machining accuracy, and machining of
 162 the whole tool path is completed by controlling tool movement from the j th tool contact point to the $j+1$ th
 163 tool contact point in an interpolation cycle[25, 26].

164 Curvature of the machined curve P_i at the tool contact point C_{ij} can be expressed as[27]:

165
$$k_{ij} = \frac{\sum_{w=wj} S'_w \times S''_{ww}}{\sum_{w=wj} S'_w{}^3} \quad (5)$$

166 In formula (5)

167
$$\begin{aligned} S'_w &= S'_u U'_w + S'_v V'_w \\ S''_{ww} &= (S''_{uu} U'_w + S''_{uv} V'_w) U'_w + S''_u U''_{ww} + (S''_{vu} U'_w + S''_{vv} V'_w) V'_w + S''_v V''_{ww} \end{aligned}$$

168 Step size can be approximately as

169
$$\Delta l = 2 \left[\left(\frac{1}{k_{ij}} \right)^2 - \left(\frac{1}{k_{ij}} - \varepsilon \right)^2 \right]^{0.5} \quad (6)$$

170 Corresponding reference W_{j+1} is

171
$$W_{j+1} = W_j + \frac{\Delta l}{\sum_{w=wj} S'_w} \quad (7)$$

172 Large diameter flat end milling tools are used as far as possible in channel groove machining to improve
 173 efficiency, but it must be less than the shortest distance L_{min} , which is between the two adjacent vanes surfaces,
 174 L_{min} can be approximated by formula (8).

175
$$L_{min} \approx \min_{i, k, n} \left(\frac{2\pi R_k - Nm_k}{2N} \right) \quad (8)$$

176 where n is the number of data points of the vane root, R_k is the radius of impeller at k data point, m_k is the
 177 thickness of vane at k data point, and N is the number of vanes.

178 3.1.2 Expanding groove process of channel

179 Inverted V-shaped expanding groove tool paths are designed along two sides of grooving path, tool paths are
 180 shown in figure 3, A_i to C_i ($i=1, \dots, n$) are expanding groove lines, and B_j ($j=1, 2, \dots, m$) is intersection points
 181 of A_i to C_i . Points on the A_i , B_j and C_i are the discrete points obtained by formula (7). The expanding groove
 182 tool path follows the order of $A_i \rightarrow B_j \rightarrow C_i$. The number of expanding groove lines is n_r :

183
$$n_r = \frac{S}{\sqrt{2R \times h}} \quad (9)$$

184 where S is arc length between boundary lines of channel rough machining in the side of outlet, R is tool
 185 radius, and h is the allowed limit of thickness residue in the depth direction of hub surface in outlet side.

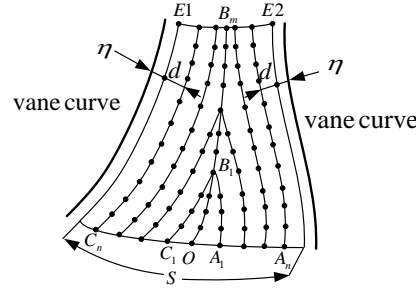


Fig. 3 Tool path of expanding groove

186 3.2 Tool path planning of vane finish machining

187 After rough machining of channel, there are some tool marks on vane profile and machining allowance is
 188 not uniform as well. Therefore, vane finish machining is carried out using five-axis side milling method, and
 189 its control points are tool location points.

190 Figure 4 shows one side of vane profile, where d_1 is finish machining curve of vane top, d_2 is finish
 191 machining curve of vane root. Point sets P_u and P_d are the discrete points of d_1 and d_2 , respectively, which
 192 are obtained by equal-parameter method. The connection curves of P_u and P_d are the generatrix of vane
 193 surface. The unit vector U_s along a generation line can be derived using equation (10).

$$194 \quad U_s = \frac{P_u - P_d}{\|P_u - P_d\|} \quad (10)$$

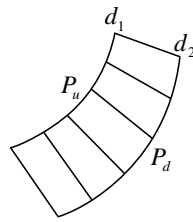


Fig. 4 Generatrix of vane finish machining surface

195 Tool location points are the coordinates of C_d point, which is obtained by offsetting a tool radius R along
 196 the normal direction of the P_d point as shown in Figure 5. Similarly, the coordinates of C_u point can be
 197 calculated as well.

$$198 \quad \begin{aligned} C_d &= P_d \pm R \cdot N_d \\ C_u &= P_u \pm R \cdot N_u \end{aligned} \quad (11)$$

199 where N_d and N_u are the unit vectors along the normal directions of P_d and P_u , respectively.

200 Cutter axes vector is computed as follows:

$$201 \quad T_t = \frac{C_u - C_d}{\|C_u - C_d\|} \quad (12)$$

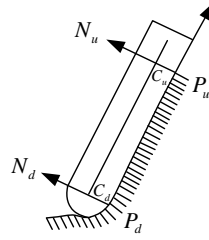


Fig.5 Cutter location and axis

202 3.3 Tool path planning of channel finish machining

203 Channel finish machining is carried out to improve machining precision and surface smoothness. Tool path
 204 is planned as one-way milling from inlet to outlet. Finish machining surface is described as a series of points
 205 according to the UV parameters orientation as shown in Figure 6. The tool path number n_f can be obtained
 206 using the equation (9). Cutter contact point $O_{u,v}$ is calculated using equation (13):

$$207 \quad O_{U,V} = O_{1,i} + \frac{O_{2,i} - O_{1,i}}{n_f} \cdot j \quad (13)$$

208 where j is the number of the cutting groove, $j=0, 1, 2, \dots, n_f$. The control method of the tool axis is the same
 209 as the channel rough machining.

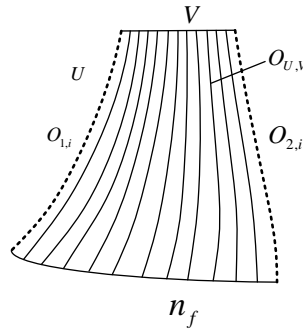


Fig. 6 Finish machining tool path

210 4. Case studies

211 A case is conducted for modeling and machining of integral impeller with eight vanes and eight channels
 212 surfaces. The top and root curve data point coordinates of vane pressure surface and suction surface of the
 213 integral impeller are listed in table 1 and table 2, respectively. The geometrical sizes of the impeller are
 214 summarized as follows: the impeller height is $75mm$, and the vane height $56mm$ with its superior margin
 215 height $17mm$.

216 **Table 1.** Data point coordinates of vane top curve

| Number | Pressure surface (mm) | | | Suction surface (mm) | | |
|--------|-----------------------|---|---|----------------------|---|---|
| | x | y | z | x | y | z |

| | | | | | | |
|---|---------|----------|----------|---------|----------|----------|
| 1 | 15.0578 | -38.5221 | -0.0000 | 17.0533 | -37.6813 | -0.0000 |
| 2 | 9.7506 | -40.4552 | -3.9523 | 11.8545 | -39.8895 | -3.9523 |
| 3 | 4.9017 | -41.9681 | -8.5921 | 7.0914 | -41.6541 | -8.5921 |
| 4 | 0.0000 | -43.9576 | -13.7361 | 3.1003 | -43.8554 | -13.7361 |
| 5 | -2.3747 | -47.3994 | -18.7416 | 0.1093 | -47.4587 | -18.7416 |
| 6 | -4.8445 | -52.5897 | -22.4812 | -2.0856 | -52.7712 | -22.4812 |
| 7 | -7.3561 | -58.6341 | -24.5000 | -4.2774 | -58.9387 | -24.5000 |

217

Table 2. Data point coordinates of vane root curve

| Number | Pressure surface (mm) | | | Suction surface (mm) | | |
|--------|-----------------------|----------|----------|----------------------|----------|----------|
| | x | y | z | x | y | z |
| 1 | 5.8562 | -15.8937 | -10.0000 | 8.5272 | -14.6354 | -10.0000 |
| 2 | 2.0282 | -20.1342 | -17.1110 | 5.2380 | -19.5435 | -17.0893 |
| 3 | -0.6451 | -25.5343 | -23.7352 | 2.7895 | -25.3057 | -23.6533 |
| 4 | -2.3108 | -32.8384 | -28.6366 | 1.1626 | -32.7485 | -28.5652 |
| 5 | -3.5795 | -41.2836 | -31.3550 | -0.2986 | -41.2614 | -31.3441 |
| 6 | -5.1602 | -50.0458 | -32.4837 | -1.6591 | -50.1741 | -32.4780 |
| 7 | -8.0303 | -58.5456 | -32.5000 | -3.9268 | -58.9631 | -32.5000 |

218 4.1 Modeling of integral impeller

219 In order to use formula (1) to generate NURBS curves of vane top and vane root, the corresponding curve
 220 control points must be obtained using their data points. First of all, a parameter value \hat{u}_k is assigned to each
 221 data point p_i , and the corresponding parameter value of the first point and the end point is specified to be 0
 222 and 1. Then the remaining parameter values \hat{u}_k are calculated one by one by the modified chord length
 223 parameter method:

$$224 \quad \hat{u}_k = \hat{u}_{k-1} + \frac{\|p_k - p_{k-1}\|}{\sum_{i=1}^m \|p_i - p_{i-1}\|} \quad k = 1, 2, \dots, m-1 \quad (14)$$

225 The most important part of curve fitting is inverse calculation of control points. Select the node vector $U =$
 226 $\{u_0, u_1, \dots, u_r\}$, where $r = n + p + 1$, thus $(m + 1) \times (m + 1)$ linear equations can be got.

$$227 \quad p_k = c(\hat{u}_k) = \sum_{i=0}^m N_{i,p}(\hat{u}_k) P_i \quad (k = 0, 1, \dots, m) \quad (15)$$

228 In the above formula, there are $(m + 1)$ unknown control point P_i . Because coefficient matrix of this
 229 equation system has the characteristics of strictly diagonal dominance, a chase method is used to quickly
 230 solve the equation system to obtain control point data. Formula (15) can be solved when node vector U is
 231 known, the node vector U is solved as follows:

$$\begin{aligned}
 u_{j+p} &= \frac{1}{p} \sum_{i=j}^{j+p-1} \hat{u}_i \quad (j=1, 2, \dots, n-p) \\
 u_0 &= u_1 = \dots = u_p = 0 \\
 u_{r-p} &= u_{r-p+1} = \dots = u_r = 1
 \end{aligned}
 \tag{16}$$

233 Take $p = 3, m = 7$, and use data in table 1-2 to obtain control point data of corresponding data points
 234 through above calculation process. The four curves in Figure 7 are obtained by the cubic NURBS curve in
 235 MATLAB.

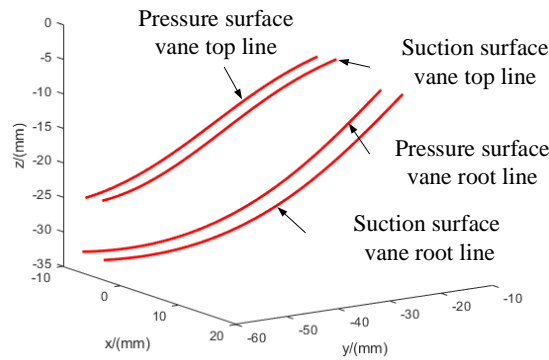


Fig. 7 Vane root and top NURBS curves

236 Vane surface is non-developable ruled surface, which is generated according to the equal parameter
 237 method by a rule line along two basic lines of a vane root line and a top line, so the scanning method is used,
 238 the parametric equation of vane ruled surface can be expressed by (17). The resulting vane surface is shown
 239 in figure 8.

$$S(u, v) = (1 - v)p(u) + vq(u)
 \tag{17}$$

241 where v is a parameter along the direction of rule line, u is a parameter along the direction of the basic line,
 242 $S(u, v)$ is the ruled surface surrounded by u and v , $p(u)$ is vane top line, $q(u)$ is vane root line.

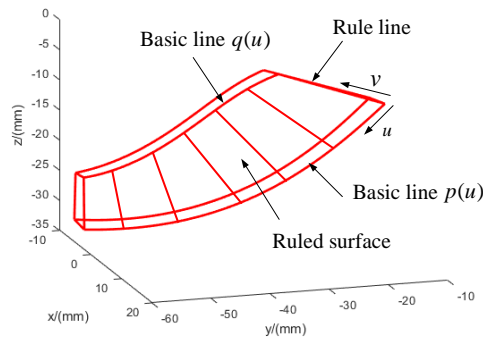


Fig.8 Non-developable ruled surface of Vane

243 Given the number of vanes is 8, the matrix is rotated according to the following spatial coordinates[28] to
 244 obtain the vanes array (see figure 9).

$$245 \begin{bmatrix} x_{rot} \\ y_{rot} \\ z_{rot} \end{bmatrix} = \begin{bmatrix} \cos \theta & -\sin \theta & 0 \\ \sin \theta & \cos \theta & 0 \\ 0 & 0 & 1 \end{bmatrix} \begin{bmatrix} x \\ y \\ z \end{bmatrix} \quad (18)$$

246 where θ is 45 degree.

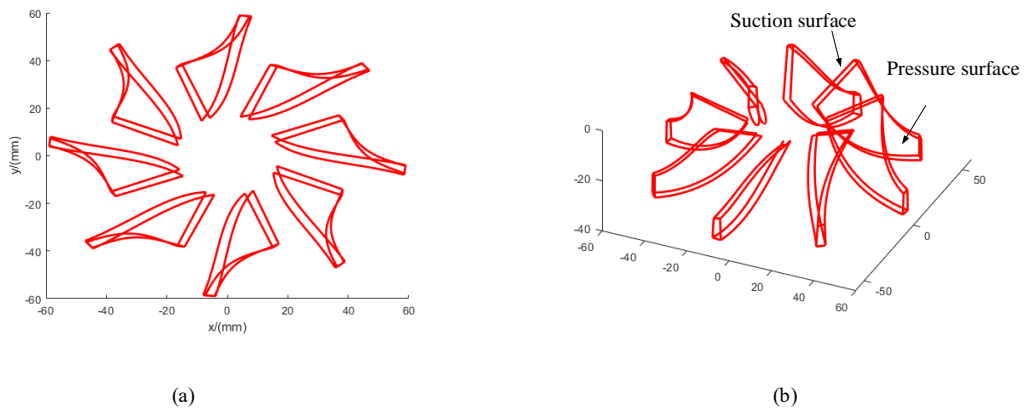


Fig. 9 Vanes generation: (a) Top view (b) Front view.

247 The scanning surface of the hub can be obtained by selecting a root curve to rotate 360 degrees around
 248 the Z axis, as shown in figure 10.

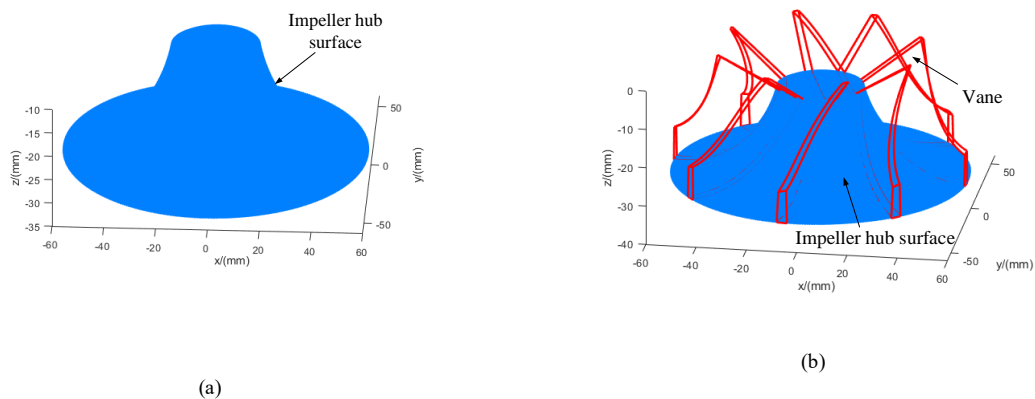


Fig. 10 Hub surface (a) Without vanes (b) With vanes

249 The data generated from MATLAB was imported into CAXA Manufacturing Engineer, and the resulting
 250 solid model is shown in figure 11.

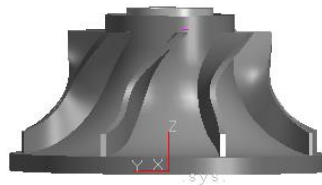


Fig.11 Integral impeller model

251 4.2 Machining of integral impeller

252 Machining of integral impeller is performed using the aforementioned tool path and processing parameters,
 253 including tool selection, parameter setting and implementation of tool path.

254 4.2.1 Selection of tools

255 In the case, flat end tools are used for grooving and expanding groove, and ball end tools are used for vane
 256 finish and channel finish. The tool material is made of kentanum. The tool diameters of the rough and finish
 257 machining are 10mm and 6mm, respectively.

258 4.2.2 Generation of Tool paths

259 The tool path for channel rough machining was first generated. On the base of impeller size and tool
 260 parameters, number of rough machining lines was calculated using equation (9) was $n_r=11$. One of them is
 261 a groove line, and the other 10 are expanding groove lines. The inverted V-type tool paths generated for
 262 rough machining of integral impeller channel were shown in Figure 12. Tool contact points and tool paths
 263 are shown in Figure 12 (a) and Figure 12 (b), respectively.



Fig.12 Generated tool path for channel roughing: (a) Tool contact points; (b) Tool paths.

264 The tool path for vane finish machining using the five-axis side milling machining method was generated.
 265 Vane allowance for finish machining was set at $0.2mm$, and channel allowance for finish machining was set
 266 at $0.5mm$. The maximum step size was set at $1mm$. The cut-in and cut-out length was set at $15mm$ to avoid
 267 interference. The path was from top to bottom. The generated tool paths are shown in Figure 13. Tool location
 268 points and tool paths are shown in Figure 13 (a) and Figure 13 (b), respectively.



Fig.13 Generated tool paths for vane finishing. (a) Tool location points; (b) Tool path.

269 According to the working conditions of the integral impeller, a set of streamlined tool path was adopted
 270 for finish machining of channel, which was milled from inlet to outlet of impeller with the vane side surface
 271 as limiting face and the hub surface as the face to be processed. To ensure machining precision, number of
 272 tool lines n_f is determined at 51 based on arc length S at the outlet of channel and formula (13). According
 273 to the step size formula (7), the calculated maximum step size is $0.3mm$. The generated tool paths of channel
 274 finish machining were shown in Figure 14.

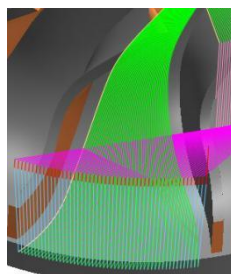


Fig.14 Generated tool paths for channel finishing

275 **5 VERICUT-based simulation verification**

276 VERICUT is a software for simulating CNC machining, which can display machining process dynamically.
277 In addition to realizing accurate mapping of real CNC machine tools, the structure and functions of virtual
278 CNC machine tools can be modified and improved for research requirement, even some new functions could
279 be added.

280 *5.1 Simulation system of machine tool*

281 A simulation system of machine tool consists two parts of mechanical subsystem model and control
282 subsystem model. 5MC850-C vertical machining center is a double turntable five-axis machining center,
283 and there are NURBS curve interpolation functions in control subsystem. The maximum strokes of machine
284 tool of X, Y, Z axis are 800mm, 500mm and 700mm, respectively. Rotation angles of A and C axis are -100°~
285 100° and -180°~ 180°, respectively, and the range of spindle speed is 100~ 18000r/min. A virtual simulation
286 system is established according to geometric dimensions and dependence relationships of 5MC850-C
287 machine center, as shown in Figure 15.

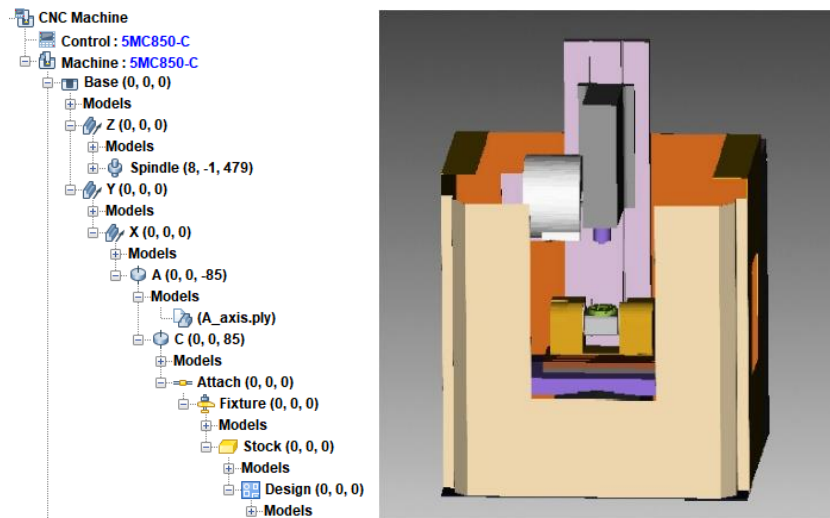


Fig.15 Simulation of machine center 5MC850-C

288 *5.2 Machining simulation*

289 The tool paths based on NURBS technology of the integral impeller are simulated in a virtual simulation
290 system of 5MC850-C machining center to verify our study. Fig.16 (a) is a simulation processing screenshot,
291 and Fig.16 (b) is a simulation screenshot of channel grooving—channel expanding groove—vane
292 finishing—channel finishing.

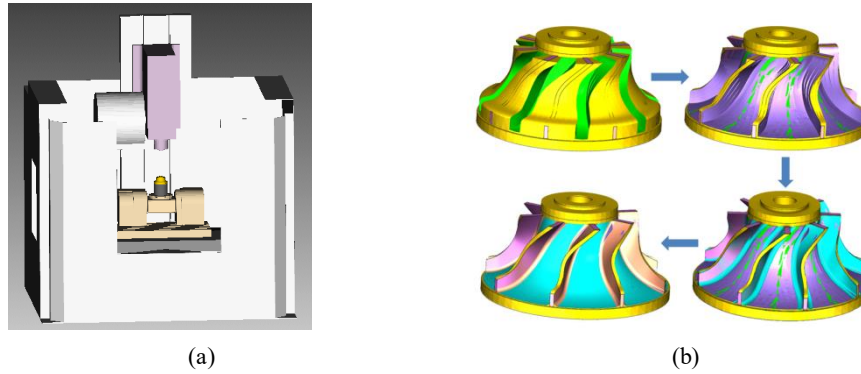


Fig.16 Simulated machining tool and simulation process. (a) Simulation machining; (b). Effect of the simulation machining.

After many times of human-computer interaction simulation, and the NC program verified by simulation is obtained. Table 3 shows some simulation parameters obtained from VERICUT after the integral impeller was simulated machined in virtual simulation system using the correct NC program. It can be calculated from the table, that the total time of integral impeller was 6 hours 38 minutes and 16 seconds, the non-machining time was 3 hours 26 minutes and 30 seconds, the total machining path length was 37.9 meters.

Table 3 Simulation parameters

| | Spindle speed (r/min) | Average feed rate (mm/min) | Total time (h:m:s) | Empty travel time (h:m:s) | Effective cutting time (h:m:s) | Distance (mm) |
|------------------|--------------------------|-------------------------------|-----------------------|------------------------------|-----------------------------------|------------------|
| Channel grooving | 4500 | 150 | 0:30:38 | 0:20:27 | 0:10:11 | 1600 |
| Expanding groove | 5000 | 200 | 1:28:31 | 0:40:24 | 0:48:07 | 13500 |
| Vane finish | 8000 | 250 | 1:00:28 | 0:40:15 | 0:20:13 | 4500 |
| Channel finish | 8000 | 250 | 3:38:39 | 1:55:24 | 1:43:15 | 18300 |

5.3 Result analysis

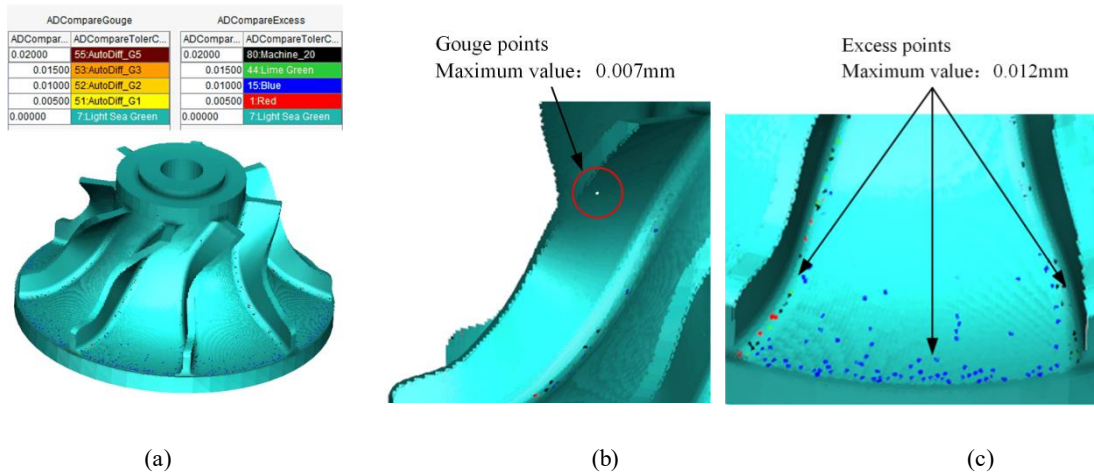
To verify feasibility of research method, dimensional accuracy of the machined impeller is checked by comparing simulation model with design model. Fig. 17 (a) shows the error distribution of the machined impeller surface, where it can be seen that there are gouge and excess at local locations, and the system indicates that there are 8 gouge points and 493 excess points on the simulated part model. Among them, gouge all occurs at the maximum variation of curvature of vane pressure surface, which main reason is that feed speed is higher when finishing machining vanes, and when the feed direction changes suddenly, the tool axis wobbles. Table 4 shows error values and coordinates of 8 gouge points, and the maximum error of 0.0067mm is shown in Fig. 17 (b). Excess points are mainly distributed in the channel outlet end and the vane root shown in Fig. 17 (c). Because the channel is narrow at the inlet and wide at the outlet, when the channel is streamlined, the residual height between the tools causes excess at the channel outlet. The excess at the vane root appears mainly due to the influence of the tool radius. The range of gouge and excess values obtained from the VERICUT is shown in Fig. (d), where the excess range was 0~0.012 mm, and the gouge

316 range was 0~0.007mm, which proves the NC program is correct and can meet the tolerance range of the
 317 impeller design.

318 **Table 4** Machining errors and coordinates of gouge points

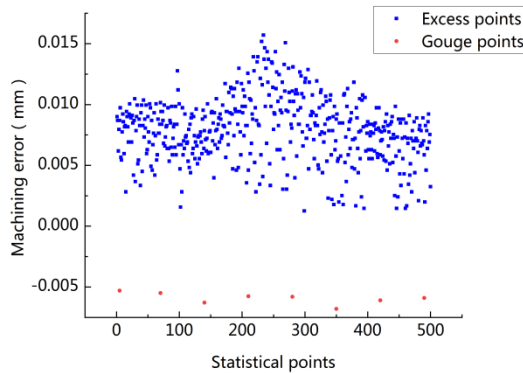
| Number | Machining error(mm) | coordinates | Number | Machining error(mm) | coordinates |
|--------|---------------------|-------------------------------|--------|---------------------|------------------------------|
| 1 | -0.0062 | (-35.7723, 22.0651, -6.0591) | 5 | -0.0057 | (35.3011, -22.4510, -6.0780) |
| 2 | -0.0055 | (-40.4927, -10.5101, -5.9223) | 6 | -0.0061 | (40.6245, -10.9631, -5.9037) |
| 3 | -0.0057 | (-22.0673, -35.7725, -6.0109) | 7 | -0.0067 | (21.0376, 36.9257, -5.9016) |
| 4 | -0.0058 | (9.9652, -40.7563, -5.9063) | 8 | -0.0055 | (-9.4253, 41.0213, -6.0452) |

319



320

321



322

323

324 Fig. 17 Error distribution and error range. (a) The machining error distribution in impeller surface. (b) Maximum gouge
 325 point. (c) Excess points distribution in flow outlet and vane root. (d) Range of gouge and excess values

326 **6. Conclusions**

327 NURBS curve is gradually becoming the only data standard of CAD/CAM. It is of great significance to
328 study the complex surface modeling and machining method based on NURBS unified curve model.

329 (1) The impeller surface modeling based on NURBS curves is realized by using MATLAB and CAXA
330 Manufacturing Engineer software, which effectively solves the problem that NURBS curves and surfaces
331 can not be directly designed in 3D CAD software.

332 (2) Flat end milling tools are used for rough machining of impeller, and grooving and expanding groove
333 are separated in channel rough machining, which not only boosts the processing efficiency but also is more
334 conducive to the release of residual stress and elastic potential energy of the blank, thus ensuring the
335 processing quality.

336 (3) The tool path of grooving and expanding groove is the NURBS curve too, and interpolation step is
337 determined jointly by the curvature of the curve and the interpolation cycle. Impeller modeling, tool path
338 and interpolation are all based on NURBS technology, which can better achieve the unified model of design
339 and manufacture.

340 (4) The verification of NC program and precision check based on simulation technology can not only
341 greatly reduce the trial cutting time of NC machine tools, but also verify the innovative design method
342 without actual machining equipment. And improve collaborative design ability.

343 At present, our work is only to study modeling and CNC machining technology of integral impeller based
344 on NURBS curves and surfaces, and obtained NC program is verified in the virtual simulation system.
345 Although our research work is all based on virtual environment and off-line, this is enough to prove our
346 research results are executable from one aspect. Of course, how to apply the research conclusions to actual
347 manufacturing is more important, it will be our next research work.

348 **Acknowledgment**

349 This work was supported by the National Science Foundation of China (Grant: 51605380), Science and
350 Technology Planning Project of Shaanxi Provincial Science and Technology Bureau's (Grant: 2016GY-019
351 and 2018JQ5086)

352

353 **References**

- 354 1. Zhang Y, Chen ZT, Zhu ZQ (2020) Adaptive machining framework for the leading/trailing edge of
355 near-net-shape integrated impeller. *Int J Adv Manuf Technol* 107:
- 356 2. Young HT, Chuang LC, Gerschwiler K, Kamps S (2004) A five-axis rough machining approach for a
357 centrifugal impeller. *Int J Adv Manuf Technol* 23:233–239
- 358 3. Song G, Li J, Sun J (2013) Analysis on prediction of surface error based on precision milling cutting
359 force model. *J Mech Eng* 49:168–170
- 360 4. Ding H, Bi QZ, Zhu LM, Xiong YL (2010) Tool path generation and simulation of dynamic cutting

- 361 process for five-axis NC machining. *Chin Sci Bull* 55:3408–3418
- 362 5. Liu Y, Shi L, Tian XC (2018) Weld seam fitting and welding torch trajectory planning based on
363 NURBS in intersecting curve welding. *Int J Adv Manuf Technol* 95:2457–2471
- 364 6. Fan W, Lee CH, Chen JH (2015) A realtime curvature-smooth interpolation scheme and motion
365 planning for CNC machining of short line segments. *Int J Mach Tools Manuf* 96:27–46
- 366 7. Chu CH, Hsieh HT, Lee CH, Yan CY (2015) Spline-constrained tool-path planning in five-axis flank
367 machining of ruled surfaces. *Int J Adv Manuf Technol* 80:2097–2104
- 368 8. Wang YH, Feng JC, Sun C, Chen M (2010) Research on Five-Axis Dual-NURBS Adaptive
369 Interpolation Algorithm for Flank Milling. In: *Key Engineering Materials*. Trans Tech Publ, pp 330–
370 335
- 371 9. Fan HZ, Wang W, Xi G (2013) A novel five-axis rough machining method for efficient manufacturing
372 of centrifugal impeller with free-form blades. *Int J Adv Manuf Technol* 68:1219–1229
- 373 10. Kim DW, Suhaimi M, Kim BM, Jang DK, Chen FF (2013) Rough Cut Machining for Impellers with
374 3-Axis and 5-Axis NC Machines. In: *Advances in Sustainable and Competitive Manufacturing
375 Systems*. Springer, pp 609–616
- 376 11. Chen KH (2011) Investigation of tool orientation for milling blade of impeller in five-axis machining.
377 *Int J Adv Manuf Technol* 52:235–244
- 378 12. Wang LY, Huang HH, West RW, Wang DZ (2014) Intelligent manufacturing system of impeller for
379 computer numerical control (CNC) programming based on KBE. *J Cent South Univ* 21:4577–4584
- 380 13. Han FY, Zhang CW, Guo W, Peng XL, Zhang W (2019) A high-efficiency generation method of
381 integral impeller channel tool path based on parametric domain template trajectory mapping. *Int J Adv
382 Manuf Technol* 100:75–85
- 383 14. Li M, Liu X, Jia D, Liang Q (2015) Interpolation using non-uniform rational B-spline for the smooth
384 milling of ruled-surface impeller blades. *Proc Inst Mech Eng Part B-J Eng Manuf* 229:1118–1130.
- 385 15. Wu JC, Zhou HC, Tang XQ, Chen JH (2015) Implementation of CL points preprocessing methodology
386 with NURBS curve fitting technique for high-speed machining. *Comput Ind Eng* 81:58–64
- 387 16. Liu Q, Liu H, Yuan SM (2016) High accurate interpolation of NURBS tool path for CNC machine
388 tools. *Chin J Mech Eng* 29:911–920
- 389 17. Yao Z, Feng JC, Wang YH (2008) Dual NURBS Curve Interpolation Algorithm for 5-axis Machining.
390 *J-SHANGHAI JIAOTONG Univ-Chin Ed*- 42:0235
- 391 18. Piegl L, Tiller W (1997) B-spline Curves and Surfaces. In: *The NURBS book*. Springer, pp 81–116

- 392 19. Shi F (2001) Computer aided geometric design and non-uniform rational B-spline. High Educ Press
393 Beijing
- 394 20. Peng J, Liu X, Si L, Liu J (2017) A Novel Approach for NURBS Interpolation with Minimal Feed Rate
395 Fluctuation Based on Improved Adams-Moulton Method. Math Probl Eng 2017:
- 396 21. Fan HZ, Xi G, Wang W, Cao YL (2016) An efficient five-axis machining method of centrifugal
397 impeller based on regional milling. Int J Adv Manuf Technol 87:789–799
- 398 22. Jung H, Kim K (2000) A new parameterisation method for NURBS surface interpolation. Int J Adv
399 Manuf Technol 16:784–790
- 400 23. Jiang D, Wang LC (2006) An algorithm of NURBS surface fitting for reverse engineering. Int J Adv
401 Manuf Technol 31:92–97
- 402 24. Ma WY, Kruth JP (1998) NURBS curve and surface fitting for reverse engineering. Int J Adv Manuf
403 Technol 14:918–927
- 404 25. Xu K, Luo M, Tang K (2016) Machine based energy-saving tool path generation for five-axis end
405 milling of freeform surfaces. J Clean Prod 139:1207–1223
- 406 26. Li L, Deng XG, Zhao JH, Zho F, Sutherland JW (2018) Multi-objective optimization of tool path
407 considering efficiency, energy-saving and carbon-emission for free-form surface milling. J Clean Prod
408 172:3311–3322
- 409 27. Tsai MC, Cheng CW, Cheng MY (2003) A real-time NURBS surface interpolator for precision three-
410 axis CNC machining. Int J Mach Tools Manuf 43:1217–1227
- 411 28. Featherstone R (1983) Position and velocity transformations between robot end-effector coordinates
412 and joint angles. Int J Robot Res 2:35–45

413

414 **Corresponding author**

415 **Juan Wei,**

416 Professor,

417 Doctor of engineering,

418 Presently working in College of Mechanical Engineering Xi'an University of Science and Technology, the
419 main research direction is modern mechanical manufacturing technology and mechatronics system design,
420 etc.

421 E-mail: juanw@xist.edu.cn, 502262445@qq.com

422 Cell phone: 86-15934836638

423 Fax: 86-029-85583159